ChemPubSoc Europe

DOI: 10.1002/chem.201503309

CHEMISTRY A European Journal Full Paper

C–C Coupling |*Hot Paper*|

On the Triple Role of Fluoride Ions in Palladium-Catalyzed Stille Reactions

Marius Hervé,[a] Guillaume Lefèvre,[b] Emily A. Mitchell,[c] Bert U. W. Maes,*[c] and Anny Jutand*[a]

Abstract: The mechanism of Stille reactions (cross-coupling of ArX with Ar′Sn*n*Bu$_3$) performed in the presence of fluoride ions is established. A triple role for fluoride ions is identified from kinetic data on the rate of the reactions of *trans*-[ArPdBr(PPh$_3$)$_2$] (Ar = Ph, *p*-(CN)C$_6$H$_4$) with Ar′SnBu$_3$ (Ar′ = 2-thiophenyl) in the presence of fluoride ions. Fluoride ions promote the rate-determining transmetallation by formation of *trans*-[ArPdF(PPh$_3$)$_2$], which reacts with Ar′SnBu$_3$ (Ar′ = Ph, 2-thiophenyl) at room temperature, in contrast to *trans*-[ArPdBr(PPh$_3$)$_2$], which is unreactive. However, the concentration ratio [F$^-$]/[Ar′SnBu$_3$] must not be too high, because of the formation of unreactive anionic stannate [Ar′Sn(F)Bu$_3$]$^-$. This rationalises the two kinetically antagonistic roles exerted by the fluoride ions that are observed experimentally, and is found to be in agreement with the kinetic law. In addition, fluoride ions promote reductive elimination from *trans*-[ArPdAr′(PPh$_3$)$_2$] generated in the transmetallation step.

Introduction

The Stille reaction is a cross-coupling reaction between aryl halides and organostannane derivatives [Eq. (1)].[1] The popularity of this reaction is based on the mild reaction conditions required to create carbon–carbon bonds. Its high functional group compatibility makes it a suitable tool to couple highly functionalised subunits in the synthesis of complex natural products.[1] In addition, organostannanes can be easily synthesised in a variety of ways and stored without special precautions.[2]

$$ArX + R'SnR_3 \xrightarrow[\text{additives}]{\text{Pd cat}} ArR' + XSnR_3 \quad (1)$$

R' = vinyl, alkynyl, aryl, heteroaryl; R = alkyl

The postulated mechanism involves at least three steps: i) oxidative addition of a [Pd^{0}L$_n$] complex with ArX to generate [ArPdXL$_n$] (n = 1 or 2), ii) transmetallation of [ArPdXL$_n$] by R′SnR$_3$, and iii) reductive elimination of ArR′ from [ArPdR′L$_n$] (n = 1 or 2).[1] Stille reactions are known to be more efficient in the presence of additives such as copper,[3] chloride[4] and fluoride anions,[5] or copper with fluorides,[6] owing to a synergetic effect. The beneficial role of CuI in Stille reactions was rationalised as a complexation of one ligand L of [ArPdXL$_2$] to CuI.[3c] The ensuing unsaturated [ArPdXL] complex would be thus more reactive in the transmetallation step with CH$_2$=CH–SnBu$_3$, allowing for coordination of a η^2-C=C bond to Pd.[3c,1e] A transfer of the R′ group of R′SnBu$_3$ to CuI to form a more reactive {R′Cu} species in the transmetallation was also disclosed.[3c,1f] We reported a dually beneficial role of chloride ions in the Stille reaction when using the precatalyst [PdCl$_2$(PPh$_3$)$_2$],[4] namely i) in situ halide metathesis in [ArPdX(PPh$_3$)$_2$] (X = I, Br) leading to [ArPdCl(PPh$_3$)$_2$], which is more reactive in the transmetallation step with organostannane derivatives, and ii) stabilisation of [Pd^0(PPh$_3$)$_2$] (formed by reduction of [PdCl$_2$(PPh$_3$)$_2$] by R′SnBu$_3$) with formation of stable anionic [Pd^{0}Cl(PPh$_3$)$_2$]$^-$, which prevents the Pd^0 decomposition that occurs in the absence of Cl$^-$. A high catalyst loading is maintained in the presence of Cl$^-$ and the catalytic reactions become faster.[4] The accelerating effect of fluoride ions in Stille reactions[5] is proposed to be due to the formation of anionic [R′SnFR$_3$]$^-$, which is assumed to be more reactive in the transmetallation step with [ArPdXL$_n$] than the neutral R′SnR$_3$.[5b,e,f] However, a triple role of fluoride ions in the Suzuki–Miyaura[7] and Hiyama reactions[8] was recently discovered. It is established that the complexes that react with the nucleophiles [Ar′B(OH)$_2$ or Ar′Si(OMe)$_3$] are not *trans*-[ArPdXL$_2$] (L = PPh$_3$; unreactive in the transmetallation step) but *trans*-[ArPdFL$_2$] generated by reaction of F$^-$ with *trans*-[ArPdXL$_2$].[7,8] However, fluoride ions exert a decelerating role at high concentrations by formation of unreactive anionic [Ar′BF$_n$(OH)$_{3-n}$]$^-$ (n = 1–3)[7] and [Ar′SiF(OMe)$_3$]$^-$[8] respectively,

[a] *M. Hervé, Dr. A. Jutand*
Ecole Normale Supérieure-PSL Research University, Département de Chimie, Sorbonne Universités-UPMC Univ Paris 06, CNRS UMR 8640 PASTEUR
24 Rue Lhomond, 75231 Paris Cedex 5 (France)
E-mail: Anny.Jutand@ens.fr

[b] *Dr. G. Lefèvre*
CEA-Saclay, DSM-IRAMIS-NIMBE-LCMCE, UMR 3685
91191 Gif Sur Yvette, Cedex (France)

[c] *Dr. E. A. Mitchell, Prof. B. U. W. Maes*
University of Antwerp
Groenenborgerlaan 171, 2020 Antwerp (Belgium)
E-mail: bert.maes@uantwerpen.be

Supporting information for this article is available on the WWW under http://dx.doi.org/10.1002/chem.201503309.

leading to two kinetically antagonistic roles of fluoride ions in the transmetallation, the rate of which is controlled by the concentration ratio $[F^-]/[Ar'B(OH)_2]$ or $[F^-]/[Ar'Si(OMe)_3]$, respectively.[7,8] In addition, in both cross-coupling reactions, fluoride ions catalyze the reductive elimination in the intermediate *trans*-$[ArPdAr'L_2]$ to form ArAr′ and $[Pd^0L_2]$.[7,8] We report herein that fluoride ions fulfil similar roles in the Stille reaction, which is in contrast with the current mechanistic view.

Results and Discussion

The model reactions starting from isolated *trans*-$[ArPdBr(PPh_3)_2]$ (**1**) and 2-thienyl-Sn*n*Bu_3 (2-ThSnBu_3, **2**; β equiv vs. **1**) in the presence of *n*Bu_4NF (α equiv vs. **1**) were performed at room temperature in DMF [Eq. (2)]. Excess PPh_3 (2 equiv vs. **1**) was used to stabilise the palladium(0) formed in [Eq. (2)] as $[Pd^0(PPh_3)_3]$ (**4**).

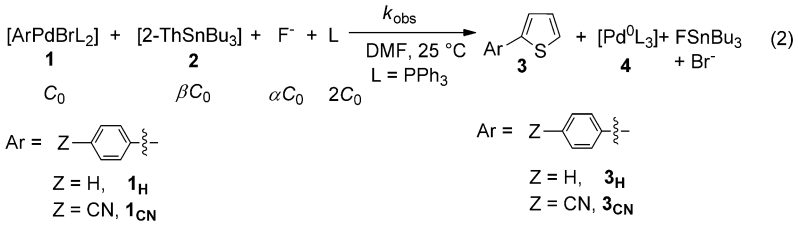

The reactions were monitored by cyclic voltammetry (CV) performed versus time.[9] Indeed, complex **4** was characterised by its oxidation peak at $E^p_{ox} = +0.05$ V vs. SCE.[10] The complexes $\mathbf{1_H}$ and $\mathbf{1_{CN}}$[11] were characterised by their reduction peaks at $E^p_{red} = -1.83$ and -1.77 V, respectively, and the cross-coupling products $\mathbf{3_H}$ and $\mathbf{3_{CN}}$ by their reduction peaks at $E^p_{red} = -2.40$ and -1.85 V, respectively, similar to those of the corresponding authentic samples.[12] Interestingly, since the reduction or oxidation currents are always proportional to the concentration of the electroactive species, their evolution with time can be easily observed.[9a]

It was first observed that *trans*-[{*p*-(CN)C_6H_4}PdBr$(PPh_3)_2$] ($\mathbf{1_{CN}}$; $C_0 = 2$ mM in DMF) did not react with 2-ThSnBu_3 (**2**) at room temperature, even in the presence of a large excess of **2** ($\beta >$ 30 equiv vs. $\mathbf{1_{CN}}$) and after a long reaction time (> 3 h; reaction performed the presence of 4 mM PPh_3). Indeed, the reduction peak current of $\mathbf{1_{CN}}$ (proportional to its concentration at any time)[9a] did not decrease with time (Figure 1a). After addition of *n*Bu_4NF ($\alpha = 6$ equiv vs. $\mathbf{1_{CN}}$) to a solution of $\mathbf{1_{CN}}$ (2 mM), **2** ($\beta = 7.5$ equiv vs. $\mathbf{1_{CN}}$) and PPh_3 (4 mM), the solution turned yellow with concomitant formation of **4** (yellow complex) and the cross-coupling product $\mathbf{3_{CN}}$, as detected by their oxidation (Figure 1b) and reduction peak (Figure 1c), respectively. The yields of **4** (99%) and $\mathbf{3_{CN}}$ (93%) were determined by considering the growth of the oxidation peak current of **4** and the reduction peak current of $\mathbf{3_{CN}}$ after addition of a known amount of authentic samples of **4** and $\mathbf{3_{CN}}$, respectively.

In a similar way, no reaction of *trans*-$[PhPdBr(PPh_3)_2]$ ($\mathbf{1_H}$; 2 mM in DMF) with 2-ThSnBu_3 ($\beta = 10$–40 equiv vs. $\mathbf{1_H}$) was observed at room temperature, in the presence of PPh_3 (4 mM; see the Supporting Information, Figure S1a). But $[Pd^0(PPh_3)_3]$ was formed in 97% yield together with $\mathbf{3_H}$ (96% yield) upon addition of F^- ($\alpha = 2.5$ equiv vs. $\mathbf{1_H}$) to a solution of $\mathbf{1_H}$ (2 mM), 2-ThSnBu_3 ($\beta = 7.5$ equiv vs. $\mathbf{1_H}$) and PPh_3 (4 mM; see the Supporting Information, Figure S1b,c). These observations confirm that the fluoride ions considerably accelerate the reaction in [Eq (2)], a key step in Stille reactions, at room temperature.

The kinetics of the reaction presented in [Eq. (2)] were monitored through the rate of formation of $[Pd^0(PPh_3)_3]$ (**4**) by chronoamperometry at a rotating disk electrode (RDE) polarised at +0.10 V vs. SCE, on the oxidation wave of **4**.[9a] The growth of the oxidation current of **4** (proportional to its concentration at time *t*) was recorded with time after addition of *n*Bu_4NF ($\alpha = 6$ vs. $\mathbf{1_H}$) to a solution of $\mathbf{1_H}$ (2 mM), **2** ($\beta = 7.5$ vs. $\mathbf{1_H}$) and PPh_3 (4 mM) in DMF at 25 °C (Figure 2a). The plot of $\ln x$ [$x = (i_{lim} - i_t)/i_{lim}$; i_{lim} is the final oxidation current of **4** and i_t is oxidation current of **4** at time *t*] versus time was linear (Figure 2b), attesting to a first-order reaction for the palladium complex: $\ln x = -k_{obs} \times t$. The observed rate constant k_{obs}, which characterised the rate of formation of $[Pd^0(PPh_3)_3]$ (the same rate as the formation of $\mathbf{3_H}$) in [Eq (2)], was calculated from the slope of the straight line (Figure 2b): $k_{obs} = 0.147$ s^{-1} (DMF, 25 °C, $\alpha = 6$, $\beta = 7.5$).

A series of similar kinetic studies were performed with varying amounts of F^- and 2-ThSnBu_3 (**2**) relative to the Pd^{II} complex $\mathbf{1_H}$ (α and β; see the Supporting Information, Figures S2–S10). The plots of k_{obs} versus α at constant β exhibited a maximum (Figure 3a). This indicates that the fluoride ions are in-

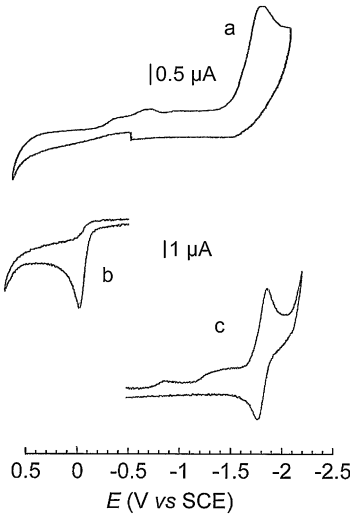

Figure 1. Cyclic voltammetry performed at a gold disk electrode ($d = 1$ mm) in DMF containing *n*Bu_4NBF_4 (0.3 M) as supporting electrolyte with a scan rate of 0.5 $V s^{-1}$ at 25 °C: a) Reduction of *trans*-[{*p*-(CN)C_6H_4}PdBr$(PPh_3)_2$] ($\mathbf{1_{CN}}$; 2 mM) in the presence of PPh_3 (4 mM). The same voltammogram is observed in the presence of 2-ThSnBu_3 (15 equiv vs. $\mathbf{1_{CN}}$); b) oxidation of $[Pd^0(PPh_3)_3]$ (**4**) formed upon addition of *n*Bu_4NF (12 mM, from a 1 M mother solution in THF) to a solution of $\mathbf{1_{CN}}$ (2 mM), 2-ThSnBu_3 (15 mM) and PPh_3 (4 mM) after 100 s; c) reduction of $\mathbf{3_{CN}}$ formed together with **4** under the experimental conditions of Figure 1b.

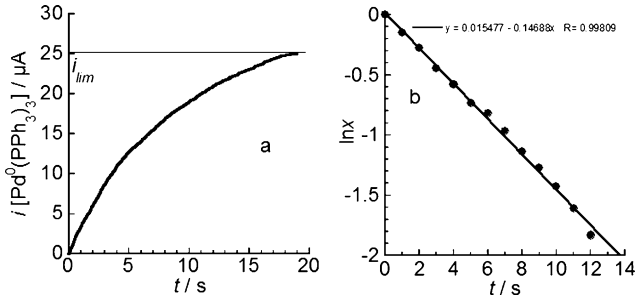

Figure 2. Kinetics of the formation of $[Pd^0(PPh_3)_3]$ (**4**) in the reaction of *trans*-$[PhPdBr(PPh_3)_2]$ ($\mathbf{1_H}$; 2 mM) with 2-$ThSnBu_3$ (7.5 equiv vs. $\mathbf{1_H}$, 15 mM) in the presence of F^- (6 equiv vs. $\mathbf{1_H}$, 12 mM) and PPh_3 (2 equiv vs. $\mathbf{1_H}$, 4 mM) in DMF at 25 °C: a) Evolution of the oxidation current i of $[Pd^0(PPh_3)_3]$ (proportional to its concentration) versus time; i was determined by chronoamperometry performed at a rotating gold disk electrode ($d = 2$ mm) polarised at +0.1 V vs. SCE; b) plot of ln x versus time: $x = (i_{lim} - i_t)/i_{lim}$; i_{lim} = final oxidation current of $[Pd^0(PPh_3)_3]$; i_t = oxidation current of $[Pd^0(PPh_3)_3]$ at time t, determined in Figure 2a.

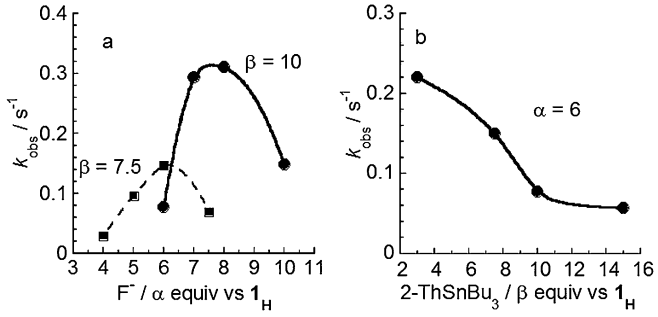

Figure 3. Kinetics of the formation of $[Pd^0(PPh_3)_3]$ (**4**) in the reaction of *trans*-$[PhPdBr(PPh_3)_2]$ $\mathbf{1_H}$ (2 mM) with 2-$ThSnBu_3$ (β equiv vs. $\mathbf{1_H}$) and F^- (α equiv vs. $\mathbf{1_H}$) in the presence of PPh_3 (4 mM) in DMF at 25 °C: a) Plot of the pseudo-first-order observed rate constant k_{obs} versus α for $\beta = 7.5$ and 10; b) plot of k_{obs} vs. β for $\alpha = 6$.

volved in two antagonistic kinetic effects. They are beneficial for the reaction at low concentration ($[F^-]/[2\text{-}ThSnBu_3] < 1$) but they exert an inhibiting effect when their concentration is too high ($[F^-]/[2\text{-}ThSnBu_3] \geq 1$; Figure 3a). A decay of k_{obs} versus β at constant α was also observed (Figure 3b). This indicates that the reaction became slower when the concentration of 2-$ThSnBu_3$ exceeded that of the fluoride ions. In other words, when $[2\text{-}ThSnBu_3]/[F^-] > 1$, the fluoride ions are quenched by 2-$ThSnBu_3$ to generate an unreactive species: anionic $[2\text{-}ThSn(F)Bu_3]^-$ [Eq. (3) in Scheme 1]. The fluorophilicity of the tin centre is well known.[13a–c] The formation of $[2\text{-}ThSn(F)Bu_3]^-$ by reaction of nBu_4NF with 2-$ThSnBu_3$ in DMF was proven by ^{19}F NMR spectroscopy ($\delta = -139.1$ ppm; see the Supporting Information, Figure S11b).[13d] Interestingly, the concentration of $[2\text{-}ThSn(F)Bu_3]^-$ increased when the initial ratio $[F^-]_0/[2\text{-}ThSnBu_3]_0$ was increased (see the Supporting Information, Table S1 and Figure S12). These experiments support the reversible formation of $[2\text{-}ThSn(F)Bu_3]^-$ in DMF [Eq. (3) in Scheme 1], the lack of reactivity of which is established in Figure 3.

The dependence of k_{obs} versus the concentration of the fluoride ions and 2-$ThSnBu_3$ indicates that $[Pd^0(PPh_3)_3]$ is formed at the same rate as $\mathbf{1_H}$ disappears. In other words, the reductive elimination from $[PhPd(2\text{-}Th)(PPh_3)_2]$ that generates $[Pd^0(PPh_3)_3]$ (the reaction order for which in 2-$ThSnBu_3$ and F^- should be zero) is faster than the transmetallation that generates $[PhPd(2\text{-}Th)(PPh_3)_2]$. Consequently, k_{obs} characterises the rate of the rate-determining transmetallation.

It has been established that fluoride ions reversibly exchange the halide of *trans*-$[ArPdX(PPh_3)_2]$ (**1**) to generate well-characterised *trans*-$[ArPdF(PPh_3)_2]$ [**5**; Eq. (4) in Scheme 1].[7a] The complex *trans*-[{*p*-$(CN)C_6H_4$}$PdF(PPh_3)_2$] ($\mathbf{5_{CN}}$) has been synthesised[7a] and submitted to reaction with 2-$ThSnBu_3$ (**2**) in the presence of PPh_3 (2 equiv vs. $\mathbf{5_{CN}}$). The reaction was monitored by cyclic voltammetry. The reduction peak of $\mathbf{5_{CN}}$ (2 mM, $E^p_{red} = -1.92$ V; see the Supporting Information, Figure S13a) rapidly disappeared after addition of **2** ($\beta = 7.5$ equiv vs. $\mathbf{5_{CN}}$) at 25 °C. $[Pd^0(PPh_3)_3]$ (**4**) was formed in 45% yield after 3 min. The expected intermediate complex *trans*-[{*p*-$(CN)C_6H_4$}Pd(2-Th)$(PPh_3)_2$] ($\mathbf{6_{CN,Th}}$) was detected at $E^p_{red} = -1.37$ V (see the Supporting Information, Figure S13b)[14] but with a low reduction peak because of the formation of **4** by reductive elimination (see the Supporting Information, Figure S13b). The products $\mathbf{3_{CN}}$ and **4** were generated in quantitative yields after 10 min (see the Supporting Information, Figure S13c,d). Since no reaction of *trans*-[{*p*-$(CN)C_6H_4$}$PdBrL_2$] ($\mathbf{1_{CN}}$) with 2-$ThSnBu_3$ was observed at the same concentrations (see above), it is thus established that the transmetallation of *trans*-*p*-$(CN)C_6H_4$-$PdFL_2$ by 2-$ThSnBu_3$ [Eq. (5) in Scheme 1] was considerably faster than that of $\mathbf{1_{CN}}$ at identical concentrations. The reaction of *trans*-$[PhPdF(PPh_3)_2]$ ($\mathbf{5_H}$)[15] (2 mM, $E^p_{red} = -2.1$ V) with 2-$ThSnBu_3$ ($\beta = 7.5$ equiv vs. $\mathbf{5_H}$) also took place within less than 3 min (as attested by the formation of **4**), confirming the following reactivity order with 2-$ThSnBu_3$, irrespective of the Ar group:

$$trans\text{-}[ArPdF(PPh_3)_2] \gg trans\text{-}[ArPdBr(PPh_3)_2]$$

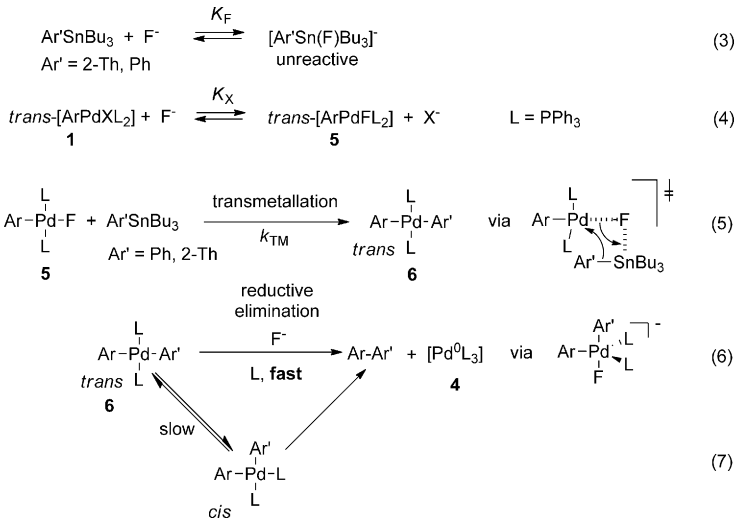

Scheme 1. Mechanism of the transmetallation and reductive elimination in Stille reactions performed in the presence of fluoride ions.

The formation of $[Pd^0(PPh_3)_3]$ when $\mathbf{5_{CN}}$ or $\mathbf{5_H}$ reacts with **2** (see above) suggests that the reductive elimination from the intermediate complexes *trans*-[{*p*-$(CN)C_6H_4$}Pd(2-Th)$(PPh_3)_2$] ($\mathbf{6_{CN,Th}}$) or *trans*-[PhPd(2-Th)$(PPh_3)_2$] ($\mathbf{6_{H,Th}}$) formed in the transmetallation took place slowly in the absence of fluoride ions, in contrast to what was observed in previous works for related complexes *trans*-[ArPdAr′$(PPh_3)_2$] (Ar = Ar′ = Ph; Ar = Ph, Ar′ = *p*-$(CN)C_6H_4$)[14] for which fluoride ions were required to promote the reductive elimination.[7] This is due to the electron-donating property of the 2-Th group in $\mathbf{6_{CN,Th}}$ and $\mathbf{6_{H,Th}}$, which favours the reductive elimination in those *trans* complexes. Indeed, it was previously established that reductive elimination in *trans*-[ArPdAr′$(PPh_3)_2$] proceeded slowly in the absence of fluoride ions when Ar or Ar′ was substituted by an electron-donating group, such as OMe[14] (interestingly, the reductive elimination in those cases was even faster in the presence of fluoride ions).[7]

The reaction of *trans*-[{*p*-$(CN)C_6H_4$}PdF$(PPh_3)_2$] ($\mathbf{5_{CN}}$; 2 mM) with $PhSnBu_3$ (36.2 equiv vs. $\mathbf{5_{CN}}$) was subsequently tested in the presence of PPh_3 (4 mM) at 25 °C. The reaction was substantially slower, indicating that $PhSnBu_3$ is less reactive than 2-ThSnBu_3. The intermediate complex *trans*-[{*p*-$(CN)C_6H_4$}PdPh$(PPh_3)_2$] ($\mathbf{6_{CN,Ph}}$) was formed and detected by its reduction peak at −1.50 V.[16] The kinetics of formation of $[Pd^0(PPh_3)_3]$ from $\mathbf{6_{CN,Ph}}$ [Eq. (6) in Scheme 1] was monitored by cyclic voltammetry (see the Supporting Information, Figure S14 b,c). The reductive elimination from $\mathbf{6_{CN,Ph}}$ was very slow (Figure 4) but was considerably accelerated upon addition of fluoride ions (6 equiv vs. $\mathbf{5_{CN}}$; Figure 4 and Figure S14 d in the Supporting Information). This is a further confirmation of what was previously established for the Suzuki[7a] and Hiyama[8] reactions: fluoride ions promote the reductive elimination from *trans*-[ArPdAr′$(PPh_3)_2$] [Eq. (6) in Scheme 1] by formation of anionic pentacoordinated palladium(II).[17] This bypasses the classical reductive elimination from the *cis* complex, which is slower due to the endergonic *trans*/*cis* isomerisation [Eq. (7) in Scheme 1].

The mechanism of the transmetallation and reductive elimination based on experimental data is shown in Scheme 1. The two antagonistic kinetic roles of the fluoride ions evidenced in Figure 3 are due to their involvement in two competitive equilibria: i) one equilibrium generates *trans*-$[ArPdFL_2]$ [Eq. (4)], which reacts with $Ar'SnBu_3$ as a consequence of the fluorophilicity of Sn [Eq. (5)]; ii) the second equilibrium generates the unreactive $[Ar'Sn(F)Bu_3]^-$ [Eq. (3)]. This mechanism is in agreement with the kinetic law [Eq. (8)] for which the theoretical variation of k_{obs} versus the fluoride concentration exhibits a maximum.[18]

$$k_{obs} = k_{TM}\beta C_o \left(\frac{1}{1 + K_F[F^-]}\right)\left(\frac{K_x[F^-]}{[X^-] + K_x[F^-]}\right) \qquad (8)$$

In addition, fluoride ions catalyse the reductive elimination from *trans*-[ArPdAr′$(PPh_3)_2$] complexes [Eq. (6)]. This leads to the catalytic cycle for the Stille reaction depicted in Scheme 2, which reveals the three different roles exerted by the fluoride ions.

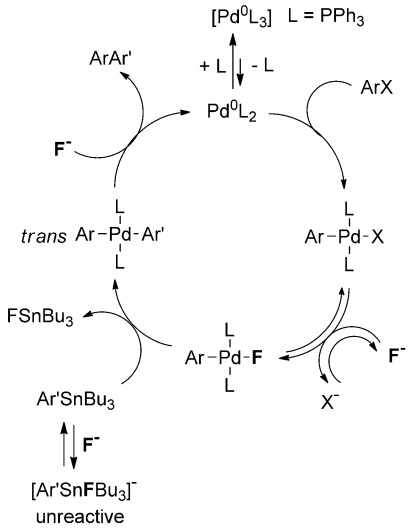

Scheme 2. Three roles for fluoride ions in the Stille reaction.

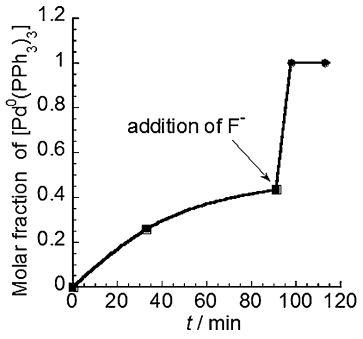

Figure 4. Kinetics of the formation of $[Pd^0(PPh_3)_3]$ (**4**) in the reaction of *trans*-[{*p*-$(CN)C_6H_4$}PdF$(PPh_3)_2$] ($\mathbf{5_{CN}}$; 2 mM) with $PhSnBu_3$ (36.2 equiv vs. $\mathbf{5_{CN}}$) until $t = 90$ min (■) and then after addition of F^- (6 equiv vs. $\mathbf{5_{CN}}$; ●). Reaction performed in the presence of PPh_3 (4 mM) in DMF at 25 °C.

The intrinsic lack of reactivity of $[2\text{-ThSn(F)Bu}_3]^-$ with *trans*-$[ArPdF(PPh_3)_2]$, established from kinetic data, can be explained by the fact that the saturated Sn centre in $[2\text{-ThSn(F)Bu}_3]^-$ is no longer fluorophilic and so cannot react with *trans*-$[ArPdF(PPh_3)_2]$ as 2-ThSnBu_3 does [Eq. (5)]. The intrinsic lack of reactivity of $[2\text{-ThSn(F)Bu}_3]^-$ with *trans*-$[ArPdBr(PPh_3)_2]$ established from kinetic data, can be easily rationalised by considering that the saturated Sn center in $[2\text{-ThSn(F)Bu}_3]^-$ cannot be bromophilic. 2-ThSnBu_3 itself has no affinity for bromide ions contrary to fluoride ions, which is why 2-ThSnBu_3 did not react with *trans*-$[ArPdBr(PPh_3)_2]$ at room temperature (see above).

DFT calculations were performed to support the lack of reactivity of the anionic $[2\text{-ThSn(F)}n\text{Bu}_3]^-$ from an electronic point of view (see the Supporting Information). Computational work was carried out by using Gaussian 09 (version B.01).[19a] Computed electron densities were analyzed by using the natural bond orbital (NBO) partition implemented in Gaussian 09.[19b] The 6-311 + G(d,p) basis set was used for all atoms (C, H, O, Si,

F, S)[19c] except Sn, which was treated by using the SDD basis set and associated pseudopotential.[19d] To take into account the London dispersion forces that can have a strong contribution to the stability of group XIV hypervalent species, the B97D functional developed by Grimme was used.[19e] This long-range dispersion-correction functional already demonstrated its efficiency in the investigation of the reactivity of silicon reagents. Solvent effects (DMF in this case) were taken into account by using the PCM model,[19f,g] also implemented in Gaussian 09. All structures were computed without geometrical constraints and were characterised as local minima (no imaginary vibration frequency).

The calculated charge repartition in $[2\text{-ThSn(F)}n\text{Bu}_3]^-$ revealed that the highest negative charge is not located on the 2-Th group but on the fluoride atom: $q(n\text{Bu}) = -0.502$ e, -0.497 e, -0.481 e; $q(\text{F}) = -0.865$ e; $q(\text{2-Th}) = -0.702$ e; $q(\text{Sn}) = +2.047$ e. This suggests that the more nucleophilic centre is the coordinated F and not 2-Th, thus explaining why $[2\text{-ThSn(F)}n\text{Bu}_3]^-$ cannot react with *trans*-$[\text{ArPdX(PPh}_3)_2]$ (X = Br, F) by direct transfer of the 2-Th group.[20a] Moreover, it is interesting to note that the anionic adduct $[2\text{-ThSn(F)}n\text{Bu}_3]^-$ incorporates a 3-center/4-electron bond (ω-bond) between the fluoride, the Sn center and the metallated C2 of the thienyl group (Figure 5). The formation of this bond can be confirmed by the presence of two occupied molecular orbitals where the electron density arising from combination of axially symmetric p orbitals (2p for C and F, and 5p for Sn) is located on F, Sn, and C2 (Ψ_1) and onto F and C2 with no contribution on Sn (Ψ_2, which only exhibits a bonding contribution between Sn and the *n*Bu groups; Figure 5).

The presence of the fluoride ion on the Sn center in $[2\text{-ThSn(F)}n\text{Bu}_3]^-$ weakens the 2-Th–Sn bond, but also fills the electronic vacant levels of Sn. This prevents the transmetallation step, in which Lewis-acidic character is required for the Sn centre to to interact with the fluoride of *trans*-$[\text{ArPdF(PPh}_3)_2]$ (Scheme 1). The decrease in the Lewis-acidic character of the Sn center in $[2\text{-ThSn(F)}n\text{Bu}_3]^-$ can be quantified by using NBO analysis: the interaction of the lone pairs of the fluoride anion with the antibonding 2-Th–Sn orbital in $[2\text{-ThSn(F)}n\text{Bu}_3]^-$ is estimated to lead to a stabilisation of approximately 24.2 kcal mol^{-1}.

A similar calculation for $[\text{PhSi(F)(OMe)}_3]^-$ also revealed that the highest negative charge is located on the F atom and the lowest on the Ph group.[20b] This helps to explain why $[\text{PhSi(F)(OMe)}_3]^-$ was also found to be unreactive with *trans*-$[\text{ArPdX(PPh}_3)_2]$ (X = Br, F).[8] $[\text{PhSi(F)(OMe)}_3]^-$ also incorporates a 3-center/4-electron bond, which confirms its lack of reactivity in the above-described transmetallation step (see the Supporting Information, Figure S15). Similarly to the tin analogue, the interaction of the occupied lone pair of the fluoride anion with the antibonding Ph–Si orbital is estimated to lead to a stabilisation of approximately 25.1 kcal mol^{-1}.

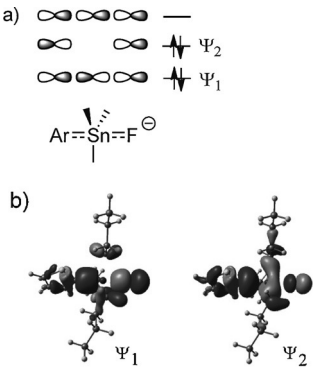

Figure 5. $[2\text{-ThSn(F)}n\text{Bu}_3]^-$: a) simplified 3-center/4-electron bond resonance arising from the interaction of 3 axially symmetric p orbitals; b) occupied 3-center/4-electron bond MOs for $[2\text{-ThSn(F)}n\text{Bu}_3]^-$. Ψ_1: HOMO−7, −0.254 eV; Ψ_2: HOMO−1, −0.189 eV. The third and empty MO resulting from the ω-bond is not represented due to the usual DFT drawbacks related to the precise computation of unoccupied levels.

Conclusion

The role of fluoride ions in the Stille reaction (cross-coupling of ArX with $\text{Ar}'\text{SnBu}_3$) has been established. Fluoride ions promote the rate-determining transmetallation by formation of more reactive *trans*-$[\text{ArPdF(PPh}_3)_2]$, which reacts with $\text{Ar}'\text{SnBu}_3$ at room temperature, in sharp contrast to unreactive *trans*-$[\text{ArPdBr(PPh}_3)_2]$. The fluoride ions also promote the reductive elimination from *trans*-$[\text{ArPdAr}'\text{(PPh}_3)_2]$ generated in the transmetallation. However, the concentration ratio $[\text{F}^-]/[\text{Ar}'\text{SnBu}_3]$ must not be too high because of the formation of unreactive anionic $[\text{Ar}'\text{Sn(F)Bu}_3]^-$. This explains the two kinetically antagonistic roles exerted by the fluoride ions. Consequently, fluoride ions play three roles in the Stille reaction, similar to those established in the mechanisms of the Suzuki and Hiyama reactions.

Experimental Section

Typical procedure for the kinetics of the reaction of *trans*-$[\text{PhPdBr(PPh}_3)_2]$ with 2-ThSnBu_3 in the presence of $n\text{Bu}_4\text{NF}$ in DMF, as monitored by chronoamperometry at a rotating disk electrode

Experiments were performed under argon atmosphere in a thermostated three-electrode cell connected to a Schlenk line at 25 °C. The counter electrode was a platinum wire of approximately 1 cm^2 apparent surface area; the reference was a saturated calomel electrode (SCE) separated from the solution by a bridge filled with 2 mL of a 0.3 M $n\text{Bu}_4\text{NBF}_4$ solution in DMF. A solution of degassed DMF (18 mL) containing $n\text{Bu}_4\text{NBF}_4$ (0.3 M) as supporting electrolyte was poured into the cell followed by *trans*-$[\text{PhPdBr(PPh}_3)_2]$ (28.3 mg, 0.036 mmol, 2 mM) and PPh_3 (18.9 mg, 0.072 mmol). 2-ThSnBu_3 (85 μL, 0.27 mmol) was then introduced into the cell. The kinetic measurements were performed at a rotating gold disk electrode ($d = 2$ mm, inserted into a Teflon holder, EDI 65109, radiometer) with an angular velocity of 105 rad s^{-1}. The rotating electrode was polarised at +0.1 V on the oxidation wave of $[\text{Pd}^0(\text{PPh}_3)_3]$. $n\text{Bu}_4\text{NF}$ (216 μL of a commercial 1 M mother solution in THF, 0.216 mmol) was then added into the cell and the increase of the oxidation current of $[\text{Pd}^0(\text{PPh}_3)_3]$ was recorded versus time up to a limit value, attesting the end of the reaction. The solution turned yellow, the color of $[\text{Pd}^0(\text{PPh}_3)_4]$ in DMF. Cyclic voltammetry at the same steady electrode was then performed towards oxidation po-

tentials and revealed the oxidation peak of $[Pd^0(PPh_3)_3]$. Its yield (97%) was determined from the increase of its oxidation peak current after addition of an authentic sample of $[Pd^0(PPh_3)_4]$ (21 mg, 0.018 mmol). A cyclic voltammetry was then performed towards reduction potentials and revealed the reversible reduction peak of 2-Th–Ph. Its yield (95%) was determined from the increase of its reduction peak current after addition of a commercially available authentic sample of 2-Th–Ph (5 mg, 0.031 mmol).

Acknowledgements

This work was supported in part by the Centre National de la Recherche Scientifique (UMR CNRS-ENS-UPMC 8640), the Ministère de la Recherche (Ecole Normale Supérieure), the Hercules Foundation, and the University of Antwerp (BOF). We thank Johnson Matthey for a loan of palladium salt.

Keywords: fluoride · kinetics · palladium · Stille reaction · transmetallation

[1] a) M. Kosugi, K. Sasazawa, T. Migita, *Chem. Lett.* **1977**, 301–302; b) D. Milstein, J. K. Stille, *J. Am. Chem. Soc.* **1978**, *100*, 3636–3638; c) V. Farina, G. P. Roth in *Advances in Metal-Organic Chemistry, Vol. 5* (Ed.: L. S. Liebeskind), JAI Press, Greenwich, CT, **1996**, pp. 1–53; d) V. Farina, V. Krishnamurthy, X. J. Scott, *Organic Reactions, Vol. 50: The Stille Reaction*, Wiley, New York, **1997**; e) C. Amatore, A. Bahsoun, A. Jutand, G. Meyer, A. Ndedi Ntepe, L. Ricard, *J. Am. Chem. Soc.* **2003**, *125*, 4212–4222; f) P. Espinet, A. M. Echavarren, *Angew. Chem. Int. Ed.* **2004**, *43*, 4704–4734; *Angew. Chem.* **2004**, *116*, 4808–4839; g) G. Eidamshaus, J. D. Birch, *Org. Lett.* **2008**, *10*, 4211–4214; h) M. M. Heravi, E. Hashemi, F. Azimian, *Tetrahedron* **2014**, *70*, 7–21; i) T. O. Ronson, J. R. Carney, A. C. Whitwood, R. J. K. Taylor, I. J. S. Fairlamb, *Chem. Commun.* **2015**, *51*, 3466–3469.

[2] For recent approaches for $Ar'SnR_3$ synthesis, see: D. Qui, H. Meng, L. Jin, S. Wang, S. Tang, X. Wang, F. Mo, Y. Zhang, J. Wang, *Angew. Chem. Int. Ed.* **2013**, *52*, 11581–11584; *Angew. Chem.* **2013**, *125*, 11795–11798.

[3] a) L. S. Liebeskind, R. W. Fengi, *J. Org. Chem.* **1990**, *55*, 5359–5364; b) G. P. Roth, V. Farina, L. S. Liebeskind, E. Pena-Cabrera, *Tetrahedron Lett.* **1995**, *36*, 2191–3194; c) V. Farina, S. Kapadia, B. Krishnan, C. Wang, L. S. Liebeskind, *J. Org. Chem.* **1994**, *59*, 5905–5911.

[4] S. Verbeeck, C. Meyers, P. Franck, A. Jutand, B. U. W. Maes, *Chem. Eur. J.* **2010**, *16*, 12831–12837.

[5] a) A. F. Littke, G. C. Fu, *Angew. Chem. Int. Ed.* **1999**, *38*, 2411–2413; *Angew. Chem.* **1999**, *111*, 2568–2570; b) G. A. Grasa, S. P. Nolan, *Org. Lett.* **2001**, *3*, 119–122; c) A. F. Littke, L. Schwarz, G. C. Fu, *J. Am. Chem. Soc.* **2002**, *124*, 6343–6348; d) W. Su, S. Urgaonkar, P. A. McLaughlin, J. G. Verkade, *J. Am. Chem. Soc.* **2004**, *126*, 16433–16439; e) A. Echavarren, *Angew. Chem. Int. Ed.* **2005**, *44*, 3962–3965; *Angew. Chem.* **2005**, *117*, 4028–4031; f) for reaction of preformed $[R'_3SnF_2]^-$, see: A. García Martínez, J. Osío Barcina, M. Colorado Heras, A. de Fresno Cerezo, *Organometallics* **2001**, *20*, 1020–1023; g) J. R. Naber, S. L. Buchwald, *Adv. Synth. Catal.* **2008**, *350*, 957–961; h) for DFT calculations on the role of fluoride ions, see: A. Ariafard, B. F. Yates, *J. Am. Chem. Soc.* **2009**, *131*, 13981–13991.

[6] a) S. P. H. Mee, V. Lee, J. E. Baldwin, *Angew. Chem. Int. Ed.* **2004**, *43*, 1132–1136; *Angew. Chem.* **2004**, *116*, 1152–1156; b) S. P. H. Mee, V. Lee, J. E. Baldwin, *Chem. Eur. J.* **2005**, *11*, 3294–3308.

[7] a) C. Amatore, A. Jutand, G. Le Duc, *Angew. Chem. Int. Ed.* **2012**, *51*, 1379–1382; *Angew. Chem.* **2012**, *124*, 1408–1411; b) C. Amatore, G. Le Duc, A. Jutand, *Chem. Eur. J.* **2013**, *19*, 10082–10093.

[8] C. Amatore, L. Grimaud, G. Le Duc, A. Jutand, *Angew. Chem. Int. Ed.* **2014**, *53*, 6982–6985.

[9] a) For the use of electrochemical techniques to investigate the mechanism of palladium-catalyzed reactions, see: A. Jutand, *Chem. Rev.* **2008**, *108*, 2300–2347; b) CV experiments require the use of a supporting electrolyte so that experiments are performed under a high ionic strength. This mimics catalytic reactions that are performed under high ionic strength due to the continuous release of halide ions from ArX in the course of the reactions. The addition of fluoride ions in noncatalytic amounts also contributes to increasing the ionic strength. One can consider that the CV experiments are performed under experimental conditions that are close to those of the catalytic reactions.

[10] C. Amatore, A. Jutand, F. Khalil, M. A. M'Barki, L. Mottier, *Organometallics* **1993**, *12*, 3168–3178.

[11] For the synthesis of $\mathbf{1_H}$ and $\mathbf{1_{CN}}$, see: P. Fitton, E. A. Rick, *J. Organomet. Chem.* **1971**, *28*, 287–291.

[12] a) $\mathbf{3_H}$ is commercially available; b) for the synthesis of $\mathbf{3_{CN}}$, see: C. Amatore, A. Jutand, S. Negri, *J. Organomet. Chem.* **1990**, *390*, 389–398.

[13] a) *Chemistry of Tin*, 2nd ed. (Ed.: P. J. Smith), Blackie Academic & Professional, London, **1997**; b) The formation of $[PhSn(F)Me_3]^-[nBu_4N]^+$ was previously suggested by Nolan and co-workers (see ref. [5b]), who reported the emergence of a new ^{19}F-containing species in ^{19}F NMR from the reaction of nBu_4NF with $PhSnMe_3$; c) for DFT calculations, see ref. [5h]; d) A ^{19}F resonance in the same range ($\delta = -137.1$ ppm) was detected for $[PhSn(F)nBu_3]^-$ with the expected patterns due to J(F,Sn) couplings, after addition of nBu_4NF to $PhSnBu_3$ (see the Supporting Information, Figure S11 a).

[14] For the characterisation of *trans*-$[ArPdAr'(PPh_3)_2]$ complexes, see: a) C. Adamo, C. Amatore, I. Ciofini, A. Jutand, H. Lakmini, *J. Am. Chem. Soc.* **2006**, *128*, 6829–6836; b) C. Amatore, A. Jutand, G. Le Duc, *Chem. Eur. J.* **2011**, *17*, 2492–2503 and Ref. [7].

[15] For the synthesis of *trans*-$[PhPdF(PPh_3)_2]$, see: M. C. Pilon, V. V. Grushin, *Organometallics* **1998**, *17*, 1774–1781.

[16] The formation of complex $\mathbf{6_{CN,Ph}}$ has already been reported, by reaction of *trans*-$[\{p\text{-}(CN)C_6H_4\}PdF(PPh_3)_2]$ with $PhB(OH)_3$ (see ref. [7a]) and with $PhSi(OMe)_3$ (see ref. [8]).

[17] For reductive elimination induced by a fifth ligand in square planar d^{10} complexes, see: a) R. Giovannini, P. Knochel, *J. Am. Chem. Soc.* **1998**, *120*, 11186–11187; b) For pentacoordinated anionic Pd^{II} complexes favouring reductive elimination, see: R. Gramage-Doria, D. Armspach, D. Matt, L. Toupet, *Chem. Eur. J.* **2012**, *18*, 10813–10816.

[18] This kinetic law was established in refs. [7a] and [8].

[19] a) M. J. Frisch, G. W. Trucks, H. B. Schlegel, G. E. Scuseria, M. A. Robb, J. R. Cheeseman, G. Scalmani, V. Barone, B. Mennucci, G. A. Petersson, H. Nakatsuji, M. Caricato, X. Li, H. P. Hratchian, A. F. Izmaylov, J. Bloino, G. Zheng, J. L. Sonnenberg, M. Hada, M. Ehara, K. Toyota, R. Fukuda, J. Hasegawa, M. Ishida, T. Nakajima, Y. Honda, O. Kitao, H. Nakai, T. Vreven, J. A. Montgomery, Jr., J. E. Peralta, F. Ogliaro, M. Bearpark, J. J. Heyd, E. Brothers, K. N. Kudin, V. N. Staroverov, R. Kobayashi, J. Normand, K. Raghavachari, A. Rendell, J. C. Burant, S. S. Iyengar, J. Tomasi, M. Cossi, N. Rega, N. J. Millam, M. Klene, J. E. Knox, J. B. Cross, V. Bakken, C. Adamo, J. Jaramillo, R. Gomperts, R. E. Stratmann, O. Yazyev, A. J. Austin, R. Cammi, C. Pomelli, J. W. Ochterski, R. L. Martin, K. Morokuma, V. G. Zakrzewski, G. A. Voth, P. Salvador, J. J. Dannenberg, S. Dapprich, A. D. Daniels, O. Farkas, J. B. Foresman, J. V. Ortiz, J. Cioslowski, D. J. Fox, Gaussian 09, revision B.01; Gaussian, Inc.: Wallingford, CT, **2010**; b) J. P. Foster, F. Weinhold, *J. Am. Chem. Soc.* **1980**, *102*, 7211–7218; c) R. Krishnan, J. S. Binkley, R. Seeger, J. A. Pople, *J. Chem. Phys.* **1980**, *72*, 650–654; d) L. von Szentpály, P. Fuentealba, H. Preuss, H. Stoll, *Chem. Phys. Lett.* **1982**, *93*, 555–559; e) S. Grimme, *J. Comput. Chem.* **2006**, *27*, 1787–1799; f) S. Miertuš, E. Scrocco, J. Tomasi, *Chem. Phys.* **1981**, *55*, 117–129; g) G. Scalmani, M. J. Frisch, B. Mennucci, J. Tomasi, R. Cammi, V. Barone, *J. Chem. Phys.* **2006**, *124*, 094107.

[20] a) Previous DFT calculations proposed the formation of $[PhPdF(PtBu_3)]$, which reacts with CH=CH–$SnMe_3$. This step is more favoured than the reaction of $[PhPdCl(PtBu_3)]$ with anionic $[CH{=}CH{-}Sn(F)Me_3]^-$ (see ref. [5h]); b) In $[PhSi(F)(OMe)_3]^-$: $q(OMe) = -0{,}639$ e, $-0{,}641$ e, $-0{,}640$ e; $q(F) = -0{,}711$ e; $q(Ph) = -0{,}549$ e.; $q(Si) = +2{,}182$ e. Similarly, in $[PhB(OH)_3]^-$ the highest negative charge is located on the OH group and the lowest on the Ph group: $q(OH) = -0.528$ e, -0.524 e, -0.523 e.; $q(Ph) = -0.444$ e.; $q(B) = +1.019$ e. This supports the fact that $[PhB(OH)_3]^-$ was also found to be unreactive with *trans*-$[ArPdX(PPh_3)_2]$ (X = Br, F; see ref. [14b]).

Received: August 20, 2015
Published online on November 9, 2015